Excess Quantum Noise Is Colored

A. M. van der Lee, M. P. van Exter, A. L. Mieremet, N. J. van Druten, and J. P. Woerdman
Huygens Laboratory, Leiden University, P.O. Box 9504, Leiden, The Netherlands
(Received 21 July 1998)

Whereas quantum noise in a laser is essentially white, we show that excess quantum noise is colored. The coloring is determined by both the geometry (nonorthogonality) and the dynamics (eigenvalues) of the eigenmodes of the laser resonator. Experimentally, we demonstrate these concepts by using nonorthogonal polarization modes. We also show that the induced correlations between the modes can be used to greatly reduce the excess quantum noise. [S0031-9007(98)07841-7]

PACS numbers: 42.50.Lc, 42.55.Lt, 42.60.Da

The fundamental lower limit to laser noise is set by inevitable spontaneous emission. This limit, which amounts to a noise level of "one photon per mode" [1], corresponds for instance to the quantum limit of the laser linewidth first derived by Schawlow and Townes [2]. Recently there has been much interest [3–9] in *excess* quantum noise (enhanced by a factor K relative to the "one photon per mode" level) due to nonorthogonality of the eigenmodes of the laser resonator [10–12]. In this case the laser behaves in many ways as if there are K noise photons in the laser mode [1]. Very large values of K due to nonorthogonal *transverse* modes have been observed recently in the quantum-limited linewidth of an unstable-cavity laser ($K_\perp \sim 500$) [3,4] and that of a (very lossy) stable-cavity laser ($K_\perp \sim 13$) [7,8]. In addition, $K_\parallel \sim 6$ [13] (due to nonorthogonal *longitudinal* modes) and $K_{\mathrm{pol}} \sim 60$ [5] (due to nonorthogonal *polarization* modes) have been observed.

In this Letter we will show, theoretically and experimentally, that excess noise is effectively colored. Specifically, we will demonstrate that the coloring is a necessary consequence of the mechanism by which excess noise appears. In a semiclassical picture the coloring can be interpreted as follows: quantum noise emitted into the other modes arrives time-delayed in the laser mode. Since it takes time for the "$K - 1$ additional noise photons" in the laser mode to develop, the extra contribution is not spectrally white. This *dynamical* aspect of excess noise implies a limitation to K: when considering short timescales, or when limited time is available for the excess noise to develop, K will be less than expected on the basis of the purely *geometric* concept of mode nonorthogonality. In addition, we demonstrate experimentally that the mode-mode correlations, caused by the above mechanism, can be used to significantly modify the amount of excess noise observed.

Theory of excess quantum noise usually deals with a linear evolution equation including the quantum noise [12]. Within the framework of semiclassical theory (i.e., treating the laser field classically) this can be written as

$$\frac{d}{dt}|x(t)\rangle = M|x(t)\rangle + |\mathcal{L}(t)\rangle. \qquad (1)$$

Here $|x(t)\rangle$ is the state vector of the optical field in the laser resonator, M is the linear operator describing the evolution and $|\mathcal{L}(t)\rangle$ is a δ-correlated Langevin noise source that takes into account the quantum noise (spontaneous emission) [14]. The Langevin noise source is assumed to be isotropic. Usually the nonlinearity due to saturation of the gain medium is neglected, but this can be easily included by starting from the nonlinear laser equations, finding the stable working point in the absence of noise and linearizing the equations around this working point, including the quantum noise. Equation (1) is a linear stochastic differential equation which can be solved by standard techniques [15]. In the case that the eigenmodes of M are nonorthogonal, excess noise shows up [12].

In short, the coloring of the excess noise can be theoretically demonstrated as follows. We expand the state vector $|x(t)\rangle$ in eigenmodes $|a_i\rangle$ of M, i.e., $|x(t)\rangle = \sum a_i(t)|a_i\rangle$. Integrating Eq. (1) and projecting onto the measured state $|m\rangle$ yields

$$\langle m|x(t)\rangle = \sum_i a_i(0)e^{\lambda_i t}\langle m|a_i\rangle + \int_0^t dt' \sum_i e^{\lambda_i(t-t')}\frac{\langle m|a_i\rangle\langle b_i|\mathcal{L}(t')\rangle}{\langle b_i|a_i\rangle}, \qquad (2)$$

where λ_i are the eigenvalues of M and $|b_i\rangle$ are the adjoint modes of operator M (i.e., the eigenmodes of the Hermitian-conjugated operator $M^\dagger$). At the right-hand side of Eq. (2) the first term represents the noise-free evolution, while the second term represents the noise. Two limits of Eq. (2) can be easily interpreted. One occurs when $t \to 0$: as $\sum_i |a_i\rangle\langle b_i|/\langle b_i|a_i\rangle = 1$ the noise into the observed state $|m\rangle$ is simply given by the direct projection, $\langle m|\mathcal{L}\rangle$. Thus for small t the noise develops with the same ("one photon per mode") strength as for the case of orthogonal modes. Another limit is when $t \to \infty$ and one assumes that there is one mode, $|a_1\rangle$ that lases, its loss being compensated by the gain, i.e., $\mathrm{Re}(\lambda_1) = 0$. This mode will then dominate and the usual noise enhancement factor is found, $K = \langle a_1|a_1\rangle\langle b_1|b_1\rangle/|\langle a_1|b_1\rangle|^2$ [12]. The two limits illustrate

that the excess noise needs time to develop, or, phrased in the frequency domain, that excess noise is colored. The noise term in Eq. (2) shows a projective factor containing inner products and an exponential factor describing the dynamics (via the eigenvalues); in the usual treatment of excess quantum noise this dynamical factor is neglected [6,9,12]. A more extensive study of this theoretical framework will be published elsewhere [16].

As an example of the coloring-by-time-delay we consider the archetype system that shows excess noise, namely the unstable-cavity laser. The quantum noise which is injected in the adjoint mode starts as the demagnifying mode of the cavity. This mode is more and more axially confined along the resonator axis during subsequent round-trips [9]. When the diffraction limit is reached, the quantum noise feeds into the magnifying mode of the cavity. Subsequently, after some more round-trips, the quantum noise spills over the outcoupling mirror and contributes to the measured laser field. During the time corresponding to the low-loss round-trips (between the injection and the spill over), the noise emitted in the adjoint mode experiences reduced loss compared to noise emitted into the lasing mode. Thus the excess noise builds up during the low-loss round-trips. The time needed for these low-loss round-trips is the origin of the coloring of the excess noise.

We have demonstrated these concepts experimentally using the polarization variety of excess quantum noise. In this case we deal with two vector modes and the dynamics is that of two (complex) mode amplitudes. Before describing the experimental results we first discuss the theory of excess noise as it applies to our experiment [see the setup in Fig. 1]. Our HeXe laser operated at a wavelength of $\lambda = 3.51\ \mu$m, for which (as for most gas lasers) the polarization-dependent saturation favors linearly polarized light ($J = 3 \rightarrow 2$) [17]. The laser cavity has two polarization anisotropies, namely a linear dichroism of magnitude A in combination with circular birefringence of magnitude Ω. The first step is to find the steady polarization state of the laser and then to linearize around this steady state. In our case there is a stable linearly polarized state for $\Omega < A$ [17]. It is useful to express the dynamics of the two complex mode amplitudes in four real variables so that we deal with a real 4×4 matrix M. A convenient choice of four real, orthogonal variables is the phase ϕ, the intensity I, the polarization orientation θ, and the polarization ellipticity χ. The matrix M then block diagonalizes into two 2×2 matrices, one block in which the phase and the ellipticity are coupled, and another block in which the intensity and the polarization orientation are coupled. It turns out that it is much easier to measure the coloring in the intensity noise than in the phase noise. Therefore we focus for the moment on the intensity noise.

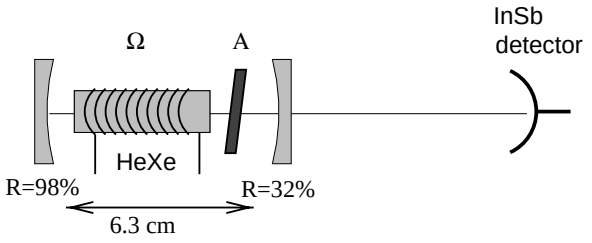

FIG. 1. Experimental setup. The HeXe laser had a stable-cavity configuration of a 98% reflecting concave gold mirror (radius of curvature 60 cm) and a 32% reflecting concave dielectric mirror (radius of curvature 30 cm) with a cavity length of 6.3 cm. A coil produces an axial magnetic field to create circular birefringence, Ω, in the HeXe gain medium. A tilted intracavity CaF_2 plate is responsible for linear dichroism, A. A cryogenic InSb detector is used to measure the output intensity.

The coupling of the intensity and the polarization-orientation fluctuations is described by

$$\frac{d}{dt}\begin{pmatrix}\delta\tilde{I}\\ \delta\theta\end{pmatrix} = \begin{pmatrix}-\beta_i I_0 & 2\Omega\\ 0 & -\gamma\end{pmatrix}\begin{pmatrix}\delta\tilde{I}\\ \delta\theta\end{pmatrix} + \begin{pmatrix}\mathcal{L}_{\tilde{I}}\\ \mathcal{L}_{\theta}\end{pmatrix}. \quad (3)$$

Here $\delta\tilde{I}$ is the normalized intensity fluctuation ($\delta I/2I_0$) [18], $\delta\theta$ is the polarization-orientation fluctuation, β_i is the polarization-isotropic part of the saturation coefficient [17], I_0 is the steady-state intensity, $\gamma = 2\sqrt{A^2 - \Omega^2}$ is the difference in damping between the two polarization eigenmodes, and $\mathcal{L}_{\tilde{I}}$ and $\mathcal{L}_{\theta}$ are uncorrelated Langevin noise sources. Mathematically, it is the off-diagonal element 2Ω which makes the eigenmodes in Eq. (3) nonorthogonal, leading to the excess intensity noise and to correlations between the polarization-orientation fluctuations and intensity fluctuations. Physically, the polarization-orientation fluctuations (caused by quantum noise into the nonlasing polarization mode) are converted into intensity fluctuations by the linear dichroism, A, with a rate which is determined by the relative angle of the polarization with respect to the linear dichroism, and the strength of the linear dichroism. The origin of the excess intensity noise can be shown explicitly by Fourier transforming Eq. (3) and calculating the power spectrum of the intensity noise:

$$\langle\delta\tilde{I}^2(\omega)\rangle = \frac{1}{\omega^2 + \beta_i^2 I_0^2}\left\{\langle\mathcal{L}_{\tilde{I}}^2(\omega)\rangle + \frac{4\Omega^2\langle\mathcal{L}_{\theta}^2(\omega)\rangle}{\omega^2 + \gamma^2}\right\}. \quad (4)$$

The intensity noise contains two terms: a direct contribution of its "own" Langevin source and an indirect contribution that stems from polarization-orientation fluctuations that are projected onto the intensity. As the Langevin noise sources ($\mathcal{L}_{\tilde{I}}$ and $\mathcal{L}_{\theta}$) have the same strength, they can be taken outside the brackets in Eq. (4), leading to a frequency-dependent enhancement factor $K(\omega) = 1 + 4\Omega^2/(\omega^2 + \gamma^2)$. In the limit $t \rightarrow 0$ (corresponding to $\omega \rightarrow \infty$) we have $K(\omega) \rightarrow 1$, so no enhancement is present, as we would expect. For $t \rightarrow \infty$ (i.e.,

$\omega \rightarrow 0$) we recover the expression for the excess noise found from mode nonorthogonality theory for this system [5], $K = A^2/(A^2 - \Omega^2)$. Note that the enhancement $K(\omega)$ is determined by the linear anisotropies Ω and A only [19], $K = 1$ for $\Omega = 0$ and $K \rightarrow \infty$ for $\Omega \rightarrow A$. The importance of Eq. (4) is that it shows that the excess noise is colored, with a bandwidth γ, due to the dynamics of the polarization-orientation fluctuations, whereas the direct quantum noise is essentially white noise [14].

In the experiment, the linear dichroism (A) was implemented by an intracavity CaF_2 glass plate, its normal tilted with respect to the resonator axis. To produce the circular birefringence (Ω) we used an axial magnetic field which induced Faraday rotation inside the HeXe gain medium. The output intensity was measured using a cryogenic InSb detector in combination with a very-low-noise home-built amplifier [noise equivalent power (NEP) ≈ 0.7 pW/$\sqrt{\text{Hz}}$] with a bandwidth of 10 MHz. The detector signal was analyzed on an rf-spectrum analyzer.

Figure 2 shows the measured frequency-resolved enhancement of the intensity noise for a fixed linear birefringence, A, and two different values of the circular birefringence, Ω. These data were obtained by normalizing the intensity-noise spectra to the spectrum for orthogonal eigenmodes, measured for $\Omega = 0$. The excess noise factor is clearly colored, the more so the larger the enhancement is. Physically, as the circular birefringence Ω is increased from zero, the damping of the polarization-orientation fluctuations (γ) decreases. A smaller γ in combination with a larger Ω results in a larger enhancement at $\omega = 0$ in combination with a stronger coloring [cf. Eq. (4)] and to a stronger coupling of the polarization-orientation noise and the intensity noise. Note the excellent agreement between theory and experiment. The dashed curves in Fig. 2 are fits to the data based upon Eq. (4). From the fits we find $A = 2.2(1)$ MHz and $\Omega/A = 0.83$ and $\Omega/A = 0.97$, respectively. The values of A and Ω can also be determined independently from the experiment using the procedure described in Ref. [5]. This results in almost the same values, namely: $A = 2.1(1)$ MHz and $\Omega/A = 0.83(2)$ and $\Omega/A = 0.97(2)$, respectively [21].

As mentioned above, the nonorthogonality of the polarization modes leads to correlations between the intensity fluctuations and polarization-orientation fluctuations. These correlations can be demonstrated explicitly by placing a polarizer in the laser output beam. After the polarizer, the polarization-orientation noise is then mixed into the intensity noise, with a strength and a phase determined by the angle between the polarizer and the steady-state polarization of the laser. Because of the correlations, mixing will lead to increased or decreased intensity noise after the polarizer, depending on whether the mixing is in phase or out of phase. Figure 3 shows intensity noise spectra obtained after a polarizer in the presence of nonorthogonal polarization modes. The data were taken under similar conditions as the upper curve in Fig. 2, but have now not been normalized to the spectrum for orthogonal modes. The peak near 10 MHz corresponds to the relaxation oscillations of the laser. The three curves correspond to different angles of the polarizer. For curve 1 of Fig. 3 the polarizer was aligned with the polarization of the laser light. In this case we observe the same spectrum as without

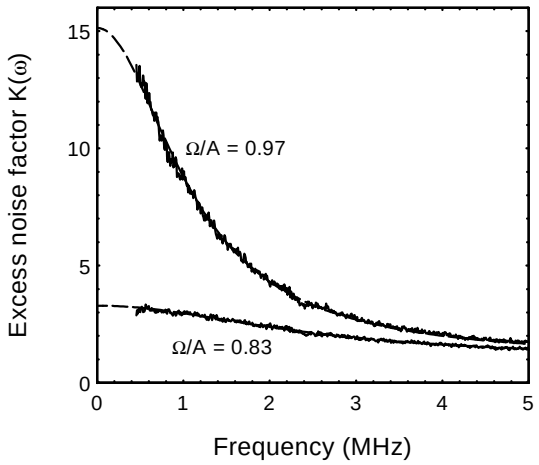

FIG. 2. Coloring of the excess quantum noise, measured in the enhancement of the intensity noise of a stable-cavity HeXe gas laser, for two different values of the nonorthogonality of the polarization eigenmodes, i.e., two different values of Ω/A. The dashed curves are fits to the experimental data. Note that the bandwidth of the coloring is smallest for the case of largest excess noise factor.

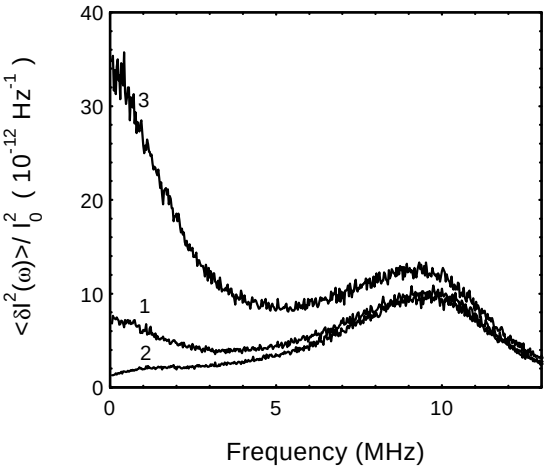

FIG. 3. Modifying the excess noise by exploiting the correlations between the polarization orientation and intensity fluctuations. The figure shows the measured intensity-noise signal after a polarizer. The different curves correspond to different angles of the transmission axis of the polarizer with respect to the polarization of the light. Curve 1: Intensity noise for parallel polarizer. Curve 2: The polarizer is rotated so as to largely cancel the excess intensity noise. Curve 3: The polarizer is rotated in the opposite direction and projects even more excess noise into the measured state.

the polarizer (since to first order, orientation fluctuations are not converted by the polarizer into intensity fluctuations). For curve 2 of Fig. 3 the polarizer was rotated by an angle of 15° from the position for curve 1, resulting in a minimum amount of excess intensity noise. For curve 3 of Fig. 3 we rotated the polarizer by the same amount, but in the opposite direction, so that the polarization-orientation noise is now mixed in with the same strength, but with opposite sign compared to curve 2. This results in even stronger excess intensity noise than in curve 1. These data show that the correlations can be used to significantly alter the amount of excess noise observed.

The reduction of excess noise can also be viewed in another way. In the space spanned by the intensity and polarization-orientation fluctuations [cf. Eq. (3)] the rotation of the polarizer changes the measured state from the eigenmode of the laser to its adjoint mode. The consequence of "projecting the laser's output on the adjoint mode" can be seen in the general formula Eq. (2): excess noise is not observed if the measured state $|m\rangle$ is the adjoint mode $|b_i\rangle$ (this follows directly from the biorthogonality relations).

We now briefly discuss the case of excess phase noise. Here it is not the polarization-orientation fluctuations that cause excess noise but the ellipticity fluctuations; these influence the phase ϕ via the circular birefringence Ω. An analysis similar to that given above yields for the power spectrum of the phase noise

$$\langle \phi^2(\omega)\rangle = \frac{1}{\omega^2}\left\{\langle \mathcal{L}_\phi^2(\omega)\rangle + \frac{4\Omega^2\langle \mathcal{L}_\chi^2(\omega)\rangle}{\omega^2 + (\gamma + \beta_a I_0)^2}\right\}, \tag{5}$$

where β_a is the polarization-anisotropic saturation coefficient [17]. As can be seen in Eq. (5) the excess phase noise is also colored, it has a bandwidth of $\gamma + \beta_a I_0$. In contrast to the intensity noise, the saturation now influences the enhancement directly, leading to a larger coloring bandwidth, $\gamma + \beta_a I_0$ instead of γ. This is due to the fact that the polarization-anisotropic saturation directly influences the damping of the ellipticity fluctuations and therefore the excess phase noise. Coloring of the phase noise is difficult to measure, as it will modify the far wings of the field spectrum. As an example, for our HeXe laser the Schawlow-Townes linewidth is typically around 1 kHz while the coloring of the phase noise is typically around 1 MHz.

To summarize, we have shown that excess quantum noise is generally colored. We have demonstrated the coloring experimentally for a two-mode system. In addition, we have used the correlations induced by mode nonorthogonality, to reduce or enhance the excess quantum noise. The coloring implies a limitation to the excess noise factor K: it appears only when sufficiently long time scales are considered. In conclusion, excess noise is not only about geometry (nonorthogonality and projection) but it involves dynamics as well.

We acknowledge support of the Stichting voor Fundamenteel Onderzoek der Materie (FOM) which is supported by NWO. The research of N. J. van Druten has been made possible by the "Koninklijke Nederlandse Akademie van Wetenschappen." We also acknowledge support from the European Union under TMR Contract No. ERB4061PL95-1021 (Microlasers and Cavity QED) and ESPRIT Contract No. 20029 (ACQUIRE).

[1] A. E. Siegman, Appl. Phys. B **60**, 247 (1995).
[2] A. L. Schawlow and C. H. Townes, Phys. Rev. **112**, 1940 (1958).
[3] Y.-J. Cheng, C. G. Fanning, and A. E. Siegman, Phys. Rev. Lett. **77**, 627 (1996).
[4] M. A. van Eijkelenborg, Å. M. Lindberg, M. S. Thijssen, and J. P. Woerdman, Phys. Rev. Lett. **77**, 4314 (1996).
[5] A. M. van der Lee *et al.*, Phys. Rev. Lett. **79**, 4357 (1997).
[6] P. Grangier and J.-P. Poizat, Eur. Phys. J. D **1**, 97 (1998).
[7] O. Emile, M. Brunel, F. Bretenaker, and A. L. Floch, Phys. Rev. A **57**, 4889 (1998).
[8] Å. M. Lindberg *et al.*, Phys. Rev. A **57**, 3036 (1998).
[9] G. H. C. New, J. Mod. Opt. **42**, 799 (1995).
[10] K. Petermann, IEEE J. Quantum Electron. **15**, 566 (1979).
[11] H. Haus and S. Kawakami, IEEE J. Quantum Electron. **21**, 63 (1985).
[12] A. E. Siegman, Phys. Rev. A **39**, 1253 (1989); **39**, 1264 (1989).
[13] S. J. M. Kuppens, M. P. van Exter, M. van Duin, and J. P. Woerdman, IEEE J. Quantum Electron. **31**, 1237 (1995).
[14] We take the Langevin noise source $|\mathcal{L}(t)\rangle$ in Eq. (1) to be δ correlated in time. This corresponds to a white noise spectrum of the quantum noise. In fact, the direct quantum noise is not completely white, the cutoff frequency being determined by the cavity loss rate and by the bandwidth of the gain medium [20]. However, for our experiment this cutoff frequency is very large (estimated as 500 MHz), so that quantum noise can be thought of as being effectively white.
[15] P. Meystre and M. Sargent III, *Elements of Quantum Optics* (Springer-Verlag, Berlin, 1991).
[16] M. P. van Exter, A. M. van der Lee, N. J. van Druten, and J. P. Woerdman (to be published).
[17] W. van Haeringen, Phys. Rev. **158**, 256 (1967). The parameters β_1 and β_2 used in this reference are directly related to our β_i and β_a: $\beta_i \propto \beta_1 + \beta_2$, $\beta_a \propto \beta_1 - \beta_2$.
[18] We divide by $2I_0$ in order to have Langevin noise sources ($\mathcal{L}_I$ and $\mathcal{L}_\theta$) of the same strength.
[19] The total enhancement is a result of a dynamical factor containing the eigenvalues and a projective factor containing the nonorthogonality [16]. In the case of Eq. (3) both factors contain the saturation ($\beta_i I_0$) but in the product the saturation dependence drops out.
[20] M. I. Kolobov, L. Davidovich, E. Giacobino, and C. Fabre, Phys. Rev. A **47**, 1431 (1993).
[21] Note that both the theoretical fit (Fig. 2) and the experimental procedure [5] are much more sensitive to the ratio of Ω/A than to the values of Ω and A separately.